

HANDBOOK OF MICROEMULSION SCIENCE AND TECHNOLOGY

edited by

Promod Kumar

*Gillette Research Institute
Gaithersburg, Maryland*

K. L. Mittal

Hopewell Junction, New York



MARCEL DEKKER, INC.

NEW YORK • BASEL

ISBN: 0-8247-1979-4

This book is printed on acid-free paper.

Headquarters

Marcel Dekker, Inc.
270 Madison Avenue, New York, NY 10016
tel: 212-696-9000; fax: 212-685-4540

Eastern Hemisphere Distribution

Marcel Dekker AG
Hutgasse 4, Postfach 812, CH-4001 Basel, Switzerland
tel: 41-61-261-8482; fax: 41-61-261-8896

World Wide Web

<http://www.dekker.com>

The publisher offers discounts on this book when ordered in bulk quantities. For more information, write to Special Sales/Professional Marketing at the headquarters address above.

Copyright © 1999 by Marcel Dekker, Inc. All Rights Reserved.

Neither this book nor any part may be reproduced or transmitted in any form or by any means, electronic or mechanical, including photocopying, microfilming, and recording or by any information storage and retrieval system, without permission in writing from the publisher.

Current printing (last digit):

10 9 8 7 6 5 4 3 2 1

PRINTED IN THE UNITED STATES OF AMERICA

2

Thermodynamics of Microemulsions I

Willem K. Kegel, J. Theo G. Overbeek, and Henk N. W. Lekkerkerker

Van't Hoff Laboratory for Physical and Colloid Chemistry, Debye Research Institute, Utrecht University, Utrecht, The Netherlands

I. INTRODUCTION

Microemulsions are thermodynamically stable mixtures of oil and water. The stability is due to the presence of fairly large amounts (several percent) of surfactants. Microemulsions are often transparent, but scattering of light, X-rays, etc. indicate that oil and water are not molecularly dispersed but are rather more coarsely mixed. By “coarse” in this case we mean that oil and water are present in domains of a few to over a hundred nanometers in size. Consequently, microemulsions contain huge oil/water interfacial areas, and to allow stability the interfacial tension must be quite low, usually $\ll 1$ mN/m. In that case the entropy of mixing, although small on account of the coarseness of the mixture, may be large enough to compensate for the positive interfacial free energy and to give the microemulsion a free energy lower than that of the unmixed components.

Microemulsions can have various textures, such as oil droplets in water, water droplets in oil, (random) bicontinuous mixtures, ordered droplets, or lamellar mixtures with a wide range of phase equilibria among them and with excess oil and/or water phases. This great variety is governed by variations in the composition of the whole system and in the structure of the interfacial layers.

Qualitatively the thermodynamics of microemulsions is well understood as the interplay between a small interfacial free energy and a small entropy of mixing. However, because of these contributions being small, other small effects, such as the influence of curvature on the interfacial tension and the influence of fluctuations, become important, and quantitative understanding still leaves a lot to be desired.

In Sec. II we discuss the mechanism by which the interfacial tension may become ultralow. After that, in Sec. III we mention curvature effects of the oil/water interface. Subsequently, a number of models for thermodynamic calculations are described (Sec. IV). In Secs. V–VII we discuss droplet-type microemulsions in some detail. Section V describes a thermodynamic formalism that incorporates the interfacial free energy (as influenced by the curvature) and the free energy of mixing of droplets and continuous medium and ultimately leads to equations for the size distribution of microemulsion droplets. This size distribution is important because measurable properties can be calculated

once it is known. In Sec. VI we discuss the quantities that determine the size distribution of the droplets, and in Sec. VII the theory of droplet-type microemulsions is compared with experiments. Finally, in Sec. VIII we discuss the main results of the theory of droplet-type microemulsions and present a short discussion of bicontinuous microemulsions and lamellar structures.

II. ULTRALOW INTERFACIAL TENSION

A. Interfacial Tension and Micelle Formation

The O/W interfacial tension (O = oil, W = water or aqueous solution) is lowered by the addition and adsorption of surfactants. The higher the concentration of the surfactant, the lower the interfacial tension, until at the cmc (critical micelle concentration) micelles are formed. Micelles are aggregates of large numbers (often 50 or more) of surfactant molecules, structured in such a way that, for a water-soluble surfactant, the hydrophobic parts of the surfactant are in the interior of the micelle, and the hydrophilic parts form its skin. As a simple consequence of mass action, nearly all surfactant added beyond the cmc forms micelles with hardly any increase in the concentration of the single molecules, and thus of their activity, which governs the adsorption and therefore the interfacial tension.

A great variety of surfactants have been used in microemulsion formation. These include common soaps, other anionic and cationic surfactants, nonionic surfactants of the polyethylene oxide type, and other structures. The hydrophobic part contains one or two linear or branched hydrocarbon chains containing about 8–18 carbon atoms. Quite often microemulsions require, in addition to oil, water, and surfactant, the presence of simple electrolytes, alcohols, and/or other weakly surface-active substances.

B. Ionic Surfactants

In many cases the interfacial tension is not yet ultralow when the cmc is reached. Schulman and collaborators [1–3], who first raised scientific interest in microemulsions, realized that the addition of a cosurfactant (e.g., a medium-sized aliphatic alcohol or amine) to an ionic surfactant (in their case soap) solved this problem by lowering the interfacial tension to virtually zero.

A good example is found in the interfacial tension between aqueous solutions of SDS (sodium dodecyl sulfate) containing 0.30 M NaCl and pentanol solutions in cyclohexane containing 0–20% pentanol [4,5] as shown in Fig. 1.

We draw attention to two aspects of these curves. At 5% pentanol the interfacial tension already reaches very low values (< 0.05 mN/m), and at 20% pentanol the curve seems to dip under the $\gamma = 0$ level. Furthermore, in the lower parts of the curves the points nearly follow a straight line, indicating, according to the Gibbs adsorption equation, Eq. (1), that the adsorption is constant (“saturation adsorption”).

$$\left(\frac{\partial \gamma}{kT \partial \ln c_{sa}} \right) = -\Gamma_{sa} \quad (1)$$

In this equation γ is the interfacial tension of the (macroscopic) oil/water interface, c_{sa} is the concentration of SDS in the aqueous phase (in molecules per unit volume), Γ_{sa} its adsorption (in molecules per unit area), and k and T have their usual meaning.

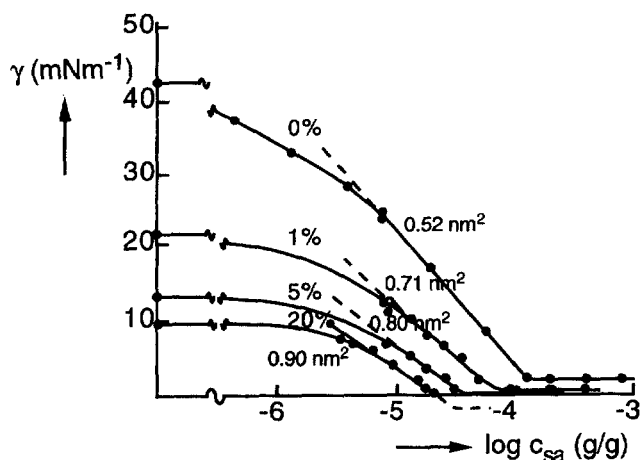


Figure 1 Interfacial tension γ as a function of the surfactant concentration c_{sa} (in g/g) between aqueous solutions of sodium dodecyl sulfate (SDS) containing 0.3 M NaCl and solutions of 0–20 wt% *n*-pentanol in cyclohexane. Without pentanol the cmc is found at about 0.0004 M SDS, and above the cmc, $\gamma = 2.42$ mN/m. Pentanol decreases the cmc and the interfacial tension above the cmc until, at 5% pentanol, γ above the cmc becomes as low as 0.036 mN/m. The area per molecule of SDS at saturation adsorption increases from 0.52 nm² in the absence of pentanol to about 0.9 nm² at 20% pentanol. Obviously the pentanol, which is adsorbed to the extent of two to three molecules per molecule of SDS, drives some of the SDS out of the interface. The experiments were carried out at 25°C.

C. Nonionic Surfactants

With nonionic surfactants of the PEO [poly(ethylene oxide)] type, the temperature is an important variable. They are water-soluble at lower temperatures and oil-soluble at high temperatures. In the narrow temperature range where the solubility changes, called PIT (phase inversion temperature [6]), the interfacial tension becomes extremely low, as sketched in Fig. 2. Below the PIT an O/W (oil-in-water) microemulsion is formed, above it a W/O (water-in-oil) microemulsion, with a continuous transition between them, possibly a bicontinuous mixture of oil and water, which at low surfactant concentrations may show a three-phase equilibrium with excess oil and water. Such equilibria are designated Winsor I (O/W + O), Winsor II (W/O + W), and Winsor III [(bicontinuous? O + W) + O + W] after P. A. Winsor [7–9], who studied phase equilibria in (mostly ionic) microemulsion systems extensively and at an early date.

D. Ionic Surfactants with Two Hydrophobic Chains

It should be mentioned here that ionic surfactants with two hydrocarbon chains do not need a cosurfactant to enable them to form microemulsions. Aerosol OT (AOT), which is sodium diethylhexylsulfosuccinate, has been known and used for a long time. In 1983 Angel et al. [10] remarked that substituted ammonium salts with two long chains, e.g., didodecyldimethylammonium bromide, would also form microemulsions without the use of a cosurfactant.

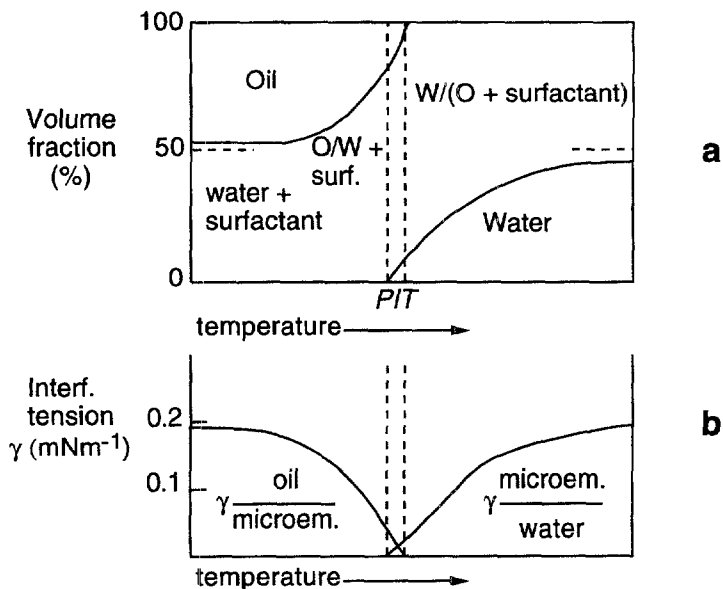


Figure 2 (a) Schematic diagram of volume fractions in a system of equal volumes of oil and water with, e.g., 5% of a PEO-type nonionic surfactant versus temperature. (b) Interfacial tensions in the same system. The line corresponding to the interfacial tension of the oil/microemulsion interface and the one corresponding to the microemulsion/water interface, are indicated. (After Ref. 6.)

E. Negative Interfacial Tension and Spontaneous Emulsification

The 20% pentanol line in Fig. 1 clearly suggests that the interfacial tension becomes negative if the surfactant concentration is increased above the concentration where $\gamma = 0$. This, however, would lead to an unstable situation, since a negative interfacial tension leads to a spontaneous increase in the area of the interface. When this happens, more surfactant will be adsorbed, thus lowering the surfactant concentration until γ is at least slightly positive. The large interfacial area thus formed may divide itself into a large number of closed shells around small droplets of either oil in water or water in oil and further decrease the free energy of the system as a direct consequence of the relatively large entropy of mixing of droplets and continuous medium. These considerations may serve as an explanation for the spontaneous formation of microemulsions that is often observed. The essential feature is that the composition of the mixture reaches $\gamma = 0$ before micelles are formed. To make this argument more quantitative we remark that the $\gamma = 0$ situation is often found at a surfactant concentration on the order of 0.1–1 wt%. Thus most of the surfactant in the mixtures will serve to make an interfacial area on the order of 1 nm² per surfactant molecule (see Sec. VI for a discussion of the order of magnitude of this molecular area), that is, on the order of 2000 m² per gram of surfactant, which is enough to stabilize 10 g of water or oil droplets with a radius of about 15 nm. So, although the surfactant is evidently the most important additive in the mixture and its amount determines the total interfacial area, it does not determine the structure of the microemulsion, not even whether it is O/W or W/O. That depends on curvature effects as discussed in the next section.

III. HOW TO AFFECT THE CURVATURE OF THE INTERFACE AND THE TYPE OF MICROEMULSION EQUILIBRIUM

Not only do surfactants and cosurfactants lower the interfacial tension, but also their molecular structures affect the curvature of the interface as shown schematically in Fig. 3. The hydrocarbon chains are rather closely packed (about 0.25 nm^2 per chain); they repel one another sideways and as a result have a tendency to bend the interface around the water side. The counterions of the ionic headgroups also repel one another sideways and thus tend to curve the interface around the oil side. The bulky polar groups of nonionic surfactants have a similar effect. So we understand qualitatively that more cosurfactant promotes W/O rather than O/W microemulsions. More electrolyte compresses the double layer, diminishes the sideways pressure of the double layer, and also promotes W/O microemulsions. The polar groups of PEO nonionics become more compact (less soluble) at higher temperatures, and so with this type of surfactants high temperature leads to W/O microemulsions.

From the above reasoning we expect that each composition of the interface has its own curvature at which the interface forms most easily and thus has the lowest interfacial tension (this interfacial tension, σ , of the droplet interface should not be confused with that of the macroscopic interface, γ). This consideration was made more quantitative by Helfrich [13], who presented an expression for the curvature free energy,

$$F_c = \int_A \left[\frac{K}{2} (c_1 + c_2 - 2c_0)^2 + \bar{K} c_1 c_2 \right] dA \quad (2)$$

as the free energy contribution due to bending of a flat interfacial area A . c_1 and c_2 are the local principal curvatures, c_0 is the spontaneous (or preferred) curvature, K is the

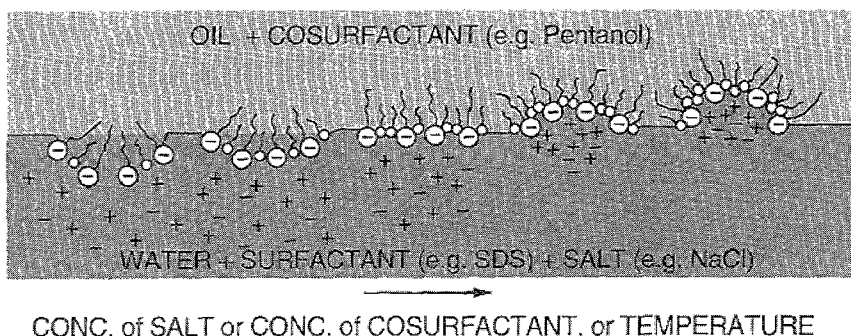


Figure 3 Schematic representation of the influence of surfactants on the curvature of the interface. The hydrophilic parts of the surfactant molecules repel each other sideways, tend to curve the interface around the oil side, and promote O/W emulsions. This effect is most pronounced with long and/or bulky nonionic polar groups or, in the case of ionic surfactants, at low electrolyte content, where the double layers are extended. On the other hand, the mutual repulsion of the hydrophobic parts of the surfactants tend to curve the interface around the water side and promote W/O emulsions. Here, long hydrocarbon tails and/or close packing, as in combinations with cosurfactants, make the effects more pronounced. (After Refs. 11 and 12.)

bending elastic modulus, and \bar{K} is the Gaussian or saddle splay modulus. $(c_1 + c_2)/2$ is referred to as “mean curvature,” while the product c_1c_2 is designated “Gaussian curvature.”

For a single droplet of radius R we have

$$F_c = 8\pi K(1 - c_0 R)^2 + 4\pi\bar{K} \quad (\text{single droplet}) \quad (3)$$

where $4\pi\bar{K}$ can be seen as the free energy needed (or furnished if \bar{K} is negative) to detach a suitable area of flat interface and close it around one droplet.

In a Winsor I or Winsor II system (generally called saturated droplet type microemulsions), the interfacial tension, σ , of the droplets can be related to the (measurable) macroscopic interfacial tension, γ , of the flat interface separating the microemulsion and the excess phase by

$$\begin{aligned} \sigma(R) &= \gamma + \int_0^{2/R} \frac{\partial \sigma(R)}{\partial (2/R)} d\left(\frac{2}{R}\right) = \gamma + \int_0^{2/R} \frac{\partial^2 F_c}{\partial A \partial (2/R)} d\left(\frac{2}{R}\right) \\ &= \gamma - \frac{4Kc_0}{R} + \frac{2K + \bar{K}}{R^2} \end{aligned} \quad (4)$$

We note that Eq. (4) does not contain finite size effects, which are expected to be present in the small systems we are dealing with here. An inclusion of such effects is postponed to Sec.V.

Figure 4 gives a schematic picture of Eq. (4), that is, the interfacial tension of the droplet interface as a function of the inverse radius of curvature, $1/R$. Curvature and radius of curvature are arbitrarily set positive for curvature around the water side (W/O) and negative for the O/W type.

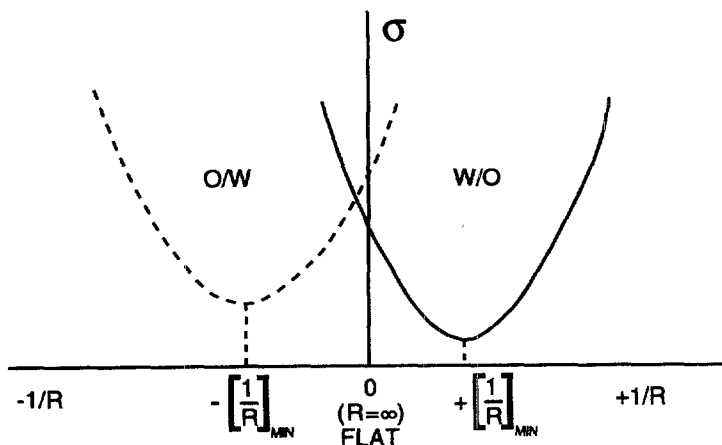


Figure 4 Tension of the droplet interface σ versus the inverse radius of curvature for two systems. In one (— — —) the repulsion between the polar groups wins and brings the “preferred” radius onto the O/W side; in the other (—) there is strong hydrophobic repulsion, and the “preferred” radius is on the W/O side.

From Eq. (4) it follows that the minimum of the interfacial tension of a droplet (the minimum in Fig. 4) is found at

$$\left(\frac{1}{R}\right)_{\text{MIN}} = \frac{2Kc_0}{2K + \bar{K}} \quad (5)$$

$(1/R)_{\text{MIN}}$ differs from c_0 due to the fact that according to Eq. (3), a term $4\pi\bar{K}$ must be added to the curvature free energy to form a droplet.

The bending elastic quantities being on the order of kT (as we show in Sec. VI), the system may increase its configurational entropy without much of a curvature free energy penalty by exploring a distribution of sizes around the one given by Eq. (5) (see Fig. 4). The entropy of mixing tends to maximize the number of droplets, and its effect is expected to result in a smaller average value of $|R|$ than the one that minimizes the curvature free energy, Eq. (5). In the case of saturated droplet-type microemulsions we may safely say that if the absolute value of the preferred curvature, c_0 , is significantly different from 0 (if not, the very presence of a microemulsion with a droplet structure may become doubtful), its sign determines whether O/W or W/O microemulsions are found. Now, as already mentioned in a more qualitative way at the beginning of this section, the sign and magnitude of c_0 are determined by two competing forces at the droplet interface: The hydrocarbon chains that tend to bend the interface around the water side contribute positively to c_0 (in our definition of the sign of the curvature), whereas the counterions of the ionic headgroups contribute negatively. At low salt concentration, for example, the contribution of the electrical double layer to the preferred curvature dominates, and an O/W system is found (Winsor I). On increasing the salt concentration, the preferred curvature becomes less and less negative and the average droplet size is found to increase. At a certain salt concentration the contributions of the electrical double layer and the hydrocarbon chains to c_0 cancel out, and a structure with a zero mean curvature is expected. In fact, many structures have zero mean curvature, not only (on average) flat monolayers but also cubic phases where (again on average) $c_1 = -c_2$ (the so-called plumber's nightmare [14]), and it is a nontrivial task to determine the stable one, especially since fluctuations around the (mean) curvature of the monolayers are expected to be present. It turns out that at low surfactant concentrations, a system consisting of a surfactant-rich middle phase coexisting with excess oil and water phases is found. The structure of the middle phase is probably bicontinuous, although it has been argued [15] that the structure might switch over rapidly from water droplets in oil to oil droplets in water. Upon increasing the salt concentration even further, c_0 becomes positive and a W/O microemulsion becomes stable, the average size of the droplets decreasing with increasing salt concentration. A similar phase inversion is found in systems where a cosurfactant is present [16]. In that case, increasing the cosurfactant concentration in the system leads to a slightly increased adsorption of cosurfactant molecules at the droplet interface, resulting in an increased surface pressure, hence a positive contribution to c_0 .

In order to proceed further, a thermodynamic formalism is needed that quantitatively relates the bending elastic quantities mentioned above to measurable properties of microemulsion systems (such as average droplet size or interfacial tension of the flat interface between the microemulsion phase and the excess oil or water phase). As a second step it is necessary to relate experimentally adjustable quantities such as the salt concentration and the nature of the surfactant to the bending elastic properties by means of molecular models. The state of the art is presented in the following sections.

IV. MODELS FOR THERMODYNAMIC CALCULATIONS

In the course of the years, several types of models have been proposed and worked out. In the early years (1940–1970) a microemulsion structure was postulated, e.g., that of isodispersed droplets of oil in water or water in oil, and the free energy of such a system was formulated from known or estimated interfacial tension and bending free energy of the monolayer as related to the overall composition of the system.

Interfacial tension and interfacial composition can be measured by performing experiments at low surfactant concentrations [see Eq. (1) and Fig. 1 for an example]. But bending free energies are much more difficult to come by, and even the entropy of mixing has posed some problems, as will be mentioned in Sec.V. In later years, starting with a paper by Talmon and Prager [17] in 1977, other models were proposed and worked out. These models are of three types:

1. Divide the total available volume into small volume elements (Voronoi polyhedra; later on, more simply, cubes were used by de Gennes and coworkers [18,19]), distribute oil and water (random distribution gives easy access to the entropy of mixing) among these volume elements, and place surfactant film at all oil/water boundaries. Choose the linear size of the volume elements equal to the persistence length [the length over which a (single) flexible film remains essentially flat]. Find the contribution of the film to the free energy from the interfacial tension and the bending free energy (caused by the difference between its average curvature as found from the model and the preferred curvature), and determine which monophasic or multiphasic situation gives the lowest value of free energy at a given total composition. An extension of this approach, where the lattice parameter is related to the ratio of the dispersed volume to the total interfacial area of the microemulsion, was put forward by Andelman et al. [20].
2. Construct an imaginary lattice (e.g., simple cubic lattice), and place O, W, and surfactant molecules on the lattice in such a way that a surfactant molecule occupies two neighboring sites—one with its polar group, the other with its hydrophobic part—and require that each lattice site contain only polar parts of molecules or hydrophobic parts of molecules. A simple example was proposed as early as 1968 by Wheeler and Widom [21], who assumed that, just as the surfactant occupies two neighboring sites, oil and water each also occupy two neighboring sites. Extending the system by adding suitable interaction energies between “oil” sites and “water” sites and making these energies dependent on the number of surfactant molecules meeting at one “oil” or one “water” site results in a model that represents the phase behavior of microemulsions in a rather realistic way as shown by several recent studies [22–24].
3. Finally, the Landau–Ginzburg approach can be applied to microemulsions. In this approach the thermodynamic behavior of a system in the neighborhood of critical points is studied. For microemulsions this approach uses the expansion of the free energy in (spatially varying) order parameter fields that are identified as the local concentration differences of oil, water, and surfactant. We will not elaborate this approach but refer to a recent review by Gompper [25].

These three theories predict the global phase behavior of microemulsion systems in terms of bending elastic properties (first approach), molecular interaction parameters (second approach), and expansion coefficients of order parameter fields (third approach). In this review, we try to fill the gap between the “early years” approach and item 1, above.

Whereas in approach I lattice models are used, we will work in the “continuum,” making extensive use of interface thermodynamics. The advantage of such an approach, as it turns out, is that detailed properties such as the size distribution of microemulsion droplets and the interfacial tension of a flat monolayer separating a microemulsion and an excess phase can be predicted. On the other hand, the lattice approaches as summarized in item 1 predict global phase behavior, which is not (yet) possible with the thermodynamic formalism reviewed in the following section. The reason is that currently a realistic model for the middle phase is lacking. A more detailed discussion regarding this issue is presented in Sec. VIII.

V. THERMODYNAMIC FORMALISM OF DROPLET-TYPE MICROEMULSIONS

A. Free Energy of Polydisperse Droplet-Type Microemulsions

We briefly review the formalism given in Ref. 26, to which the reader interested in the details of the derivation is referred. We do, however, use a different expression for the entropy of mixing. We note that the result [cf. Eq. (7)] can also be derived starting with the droplet partition function [27]. The Gibbs free energy of a droplet-type microemulsion can immediately be written in two equivalent ways as

$$G = \sum_i N_i \mu_i = \sum_i N_{im} \mu_i + \sum_j N_{dj} \mu_{dj} \quad (6)$$

where N_i and μ_i are the number of molecules and the chemical potential of the components i making up the microemulsion. In the second step in Eq. (6) we have implicitly defined droplets of category j , where j refers to the number of surfactant molecules at the interface between a droplet and the continuous medium. Of course, other definitions of droplet categories are possible. The chosen definition assumes rapid exchange of oil and water molecules but a relatively slow exchange of the surfactant molecules. The subscript im in Eq. (6) refers to component i in the continuous medium phase, while the subscript dj refers to a droplet of category j . n_{dj} and μ_{dj} are the number of droplets of category j and their chemical potential, respectively.

The droplets are considered to also include the adsorption layers. For a detailed discussion in terms of the Gibbs surface between the droplets and the medium, the reader is referred to Ref. 28.

The Gibbs free energy can also be written by first considering the system in a reference state where the microemulsion droplets are hanging on microsyringes. The free energy of the system then equals the sum of the bulk free energies of the two different “phases,” i.e., a “phase” of droplets and a “phase” of continuous medium, plus the interfacial free energy. An additional contribution to the free energy of the system arises once the droplets are allowed to move freely in the continuous medium (and the assignment “phase” as used above for the droplets and medium ceases to have meaning). This term is the free energy of mixing, which quantifies the number of additional configurations of the system due to the release of the droplets from the microsyringes. So we finally have

$$G = \sum_i N_{im} \mu_{im}^* + \sum_j \sum_i N_{ij} \mu_{ij}^* - \sum_j \Delta p_j V_{dj} + \sum_j \sigma_j A_j - TS_{\text{mix}} \quad (7)$$

where the μ^* s are the chemical potentials of the different components at the pressures inside the two different phases. The subscript im again refers to the medium, and the subscript ij refers to component i inside all droplets of category j . In the present formulation we have

assumed implicitly that all adsorbed molecules belong to the droplet. Δp_j is the difference between the pressure in the interior of a droplet of category j and the outer pressure, V_{dj} is the volume of all droplets of category j , and σ_j and A_j are the interfacial tension and interfacial area, respectively, of (all) droplets of category j . The last term (negative sign included) in Eq. (7) is the free energy of mixing, and S_{mix} the entropy of mixing. Equation (7) is most easily derived by first defining the Helmholtz free energy, since the two phases are at different pressures.

It is worth paying a little attention to the last term in Eq. (7). Neglecting excluded volume effects, the number of additional configurations of the droplets upon their release from their fixed positions is

$$\Omega = \prod_j \frac{1}{n_{dj}!} \left(\frac{V}{l^3} \right)^{n_{dj}}$$

with V the volume of the microemulsion phase and l the length over which a droplet should be translated in order to be counted as a new configuration. This is equivalent to the collection of droplets residing on a cubic lattice with lattice parameter l . Using the definition $S_{\text{mix}} = k \ln \Omega$ and taking the thermodynamic limit, the entropy of mixing becomes

$$S_{\text{mix}} = -k \sum_j n_{dj} [\ln(\rho_j l^3) - 1] = -k \sum_j n_{dj} \left[\ln \phi_j - 1 - \ln \left(\frac{v_{dj}}{l^3} \right) \right] \quad (8)$$

with ρ_j the number density of droplets of category j , ϕ_j their volume fraction, and v_{dj} the volume of a single droplet of category j .

The first equality of Eq. (8) is of the same form as the negative free energy of an ideal gas (where the summation is over only a single category) divided by temperature, with the de Broglie wavelength replaced by the length l . The fundamental difference between these two lengths is that the first is a momentum space quantity, while the second is to be evaluated in configuration space only. This evaluation is quite a subtle problem, as may be judged from the many choices that are (usually implicitly) made for this quantity, i.e., from the de Broglie wavelength of a drop [29] to the full size of a drop [20,30]. The treatment in Ref. 31 is based on the idea that the length l as defined in configuration space should be consistent with the full entropy of the system as defined in phase space. In other words, one must be careful not to either overcount or underestimate the number of additional configurations of the system that occur when the droplets are released from their fixed positions. In Ref. 31 an estimate of l is made by analyzing models that can be evaluated in full phase space and subsequently comparing the result to the definition of mixing entropy given by Eq. (7) for the same model. It turns out that the length l as defined by Eqs. (7) and (8) is on the order of the cube root of a molecular volume. This value is consistent with the one estimated much earlier [32] for microemulsion systems that were assumed to be monodisperse. In that estimate, l^3 was found to be equal to the molecular volume of the continuous phase.

We note that the calculation of mixing entropy transcends the microemulsion field and is relevant also to phenomenological theories of nucleation. In that field the length l appears in the ‘‘replacement free energy problem’’ (see Ref. 33 and, more general, Ref. 34).

It was stressed in the Introduction that microemulsions can exist because of the compensation for a small positive interfacial free energy by a small negative free energy of mixing. Here we are at a point where we can give some idea of how small is small. Taking droplets with an average radius of 10 nm at a volume fraction of 1%, assuming that most

of the volume is spread among droplets between 8 nm ($j \approx 800$) and 12 nm ($j \approx 1800$), and assuming that $l = 0.5$ nm, we find a free energy of mixing per droplet of about $20 kT$. This requires the interfacial tension σ to remain below 0.06 mN/m (say below 0.1 mN/m) to satisfy the relation $\sigma A < TS_{\text{mix}}$.

In Eqs. (7) and (8), droplet categories are defined by their number of adsorbed surfactant molecules. The only constraint in our model is that the droplets are spherical *on average*. Shape fluctuations are, at least in part, taken into account by the interfacial tension of the droplets. The analog of shape fluctuations on a flat interface is the capillary wave spectrum, the free energy of which is part of the interfacial free energy. Therefore, treating all configurations corresponding to different shapes of the droplets (i.e., counting all spherical harmonic modes) explicitly in our model leads to redundancies. However, there may be finite size effects due to the fact that not all (spherical analogs of) capillary wave modes are available for the droplets. In the next section we discuss how to implement this effect.

B. Size Distribution

The size distribution of the droplets [in the form of values of the individual ϕ_j 's; cf. Eq. (19)] is obtained by minimizing the free energy, Eqs. (6)–(8). This will be done by applying the law of mass action. The chemical potential of a droplet of category j is calculated from Eq. (7), where use is made of the generalized Laplace equation. This chemical potential is subsequently equated to the chemical potential following from mass action; i.e., it should equal the sum of the products of the number of molecules and their respective chemical potentials for all components making up a droplet. In order to find the chemical potential of the droplet categories we first need to specify the pressure differences between the droplets and the outer pressure as well as the chemical potentials of the components. The first is given by the generalized Laplace equation,

$$\Delta p_j = \frac{2\sigma_j}{R_j} - \frac{2c_j}{R_j^2} \quad (9)$$

where R_j is the radius of a drop of category j and the bending force c_j is

$$c_j = \left(\frac{\partial \sigma}{\partial (2/R)} \right)_{R=R_j} = -2Kc_0 + \frac{2K + \bar{K}}{R_j} \quad (10)$$

where we have used Eq. (4). A straightforward derivation of Eq. (9) from mechanical equilibrium is given in Ref. 28. Before proceeding further, it is useful to specify the total interfacial area of the system as

$$\sum_j A_j = \sum_j n_{dj} 4\pi R_j^2 \quad (11)$$

and the total volume of the droplets of category j as

$$V_{dj} = n_{dj} \frac{4}{3} \pi R_j^3 = \sum_i N_{ij} v_i \quad (12)$$

where v_i is the molecular volume of component i . The volume fraction of droplets of category j is given as

$$\phi_j = \frac{4}{3} \pi R_j^3 \frac{n_{dj}}{V} = \frac{V_{dj}}{\sum_j V_{dj} + \sum_i N_{im} v_i} \quad (13)$$

The chemical potentials of the components in the continuous medium now follow from Eq. (7) with Eqs. (11)–(13).

$$\mu_i = \left(\frac{\partial G}{\partial N_{im}} \right)_{T,p,N_{jm \neq im}} = \mu_{im}^* - kT \frac{\sum_j n_{dj}}{V} v_i \quad (14)$$

so that

$$\sum_{im} N_{im} \mu_i = \sum_i N_{im} \mu_{im}^* - kT \sum_j n_{dj} \quad (15)$$

where a term linear in the total volume fraction of the droplets has been dropped. From this equation together with Eq. (7) it follows that, at constant n_{dk} ($k \neq j$),

$$\mu_{dj} = \frac{\partial G}{\partial n_{dj}} = \sum_i \frac{N_{ij} \mu_{ij}^*}{n_{dj}} + \frac{4}{3} \pi R_j^2 \left(\sigma_j + \frac{2c_j}{R_j} \right) + kT \left[\ln \phi_j - \ln \left(\frac{v_{dj}}{l^3} \right) \right] \quad (16)$$

For the components making up the droplets we have

$$\mu_{ij}^* = \mu'_i + \int_p^{p+\Delta p_j} \frac{\partial \mu_i}{\partial p} dp = \mu'_i + \Delta p_j v_i = \mu'_i + \left(\frac{2\sigma_j}{R_j} - \frac{2c_j}{R_j^2} \right) v_i \quad (17)$$

where we have used Eq. (9). μ'_i is the chemical potential of the droplet components at pressure p . Putting μ_{dj} from Eq. (16) equal to the chemical potential of the droplets following from mass action, that is,

$$\mu_{dj} = \sum_i \frac{N_{ij}}{n_{dj}} \mu_i \quad (18)$$

eliminating μ_{ij}^* with Eq. (17) and making use of Eq. (12) for the droplet components, we arrive at the size distribution

$$\phi_j = \frac{v_{dj}}{l^3} \exp \left[- \frac{(4/3)\pi R_j^3 \Delta \bar{\mu} + 4\pi R_j^2 \sigma_j}{kT} \right] \quad (19)$$

with $\Delta \bar{\mu} = (\mu'_i - \mu_i)/v_i$, where the numerator is the difference between the chemical potentials of the components inside the droplets and that in a noncolloidal phase of these components, both at pressure p . It was shown in Ref. 28 that, at least for monodisperse systems, $(\mu'_i - \mu_i)/v_i$ does not depend on i . We assume that this remains true for the polydisperse microemulsion systems considered here. This requires that the compositions of the solutions in all the droplets and in a non-colloidal phase of these components be identical and that $\Delta \bar{\mu} = 0$ in order to obtain a microemulsion in equilibrium with an excess phase of the same composition as the droplet interiors. We are particularly interested in these kinds of systems, as in that situation the amount of dispersed phase and the average size of the globules are “chosen” by the system, i.e., not determined by the total volume of available dispersed phase, at least when this volume is large enough.

In Sec. III it was shown that if it is assumed that the interfacial tension of the droplets depends on curvature as prescribed by Eq. (4), then some essential features of microemulsion systems can already be qualitatively understood. In Ref. 27 the opposite route was followed. It was assumed that the interfacial tension does *not* depend on curvature, and in that case severe inconsistencies between theory and experiments were observed. As also mentioned in Sec. III, Eq. (4) does not account for finite size effects. We take into account both curvature dependence and finite size effects by using the Ansatz for the interfacial

tension,

$$\sigma(R_j) = \gamma - \frac{4Kc_0}{R_j} + \frac{2K + \bar{K}}{R_j^2} + z'kT \frac{\ln(j)}{4\pi R_j^2} \quad (20)$$

The first three terms on the right follow from Helfrich's free energy expansion in the curvature [13] as discussed in Sec. III of this chapter and are identical to the right-hand side of Eq. (4). The last term quantifies the finite size effect as mentioned at the end of Sec. V.A. It was introduced by Fisher [35] in his treatment of condensation and is widely used in phenomenological theories of nucleation (see, e.g., Refs. 36 and 37). z' has an estimated value on the order of 1. We note that the calculation of z' from a model is far from trivial; see, for example, Ref. 38 for a discussion of the relatively simple case of on average flat interfaces.

Combining Eqs. (19) and (20) and setting $\Delta\bar{\mu} = 0$, the size distribution for a saturated droplet-type microemulsion can be written as

$$\phi_j = Cj^z \exp(\tilde{c}_0 j^{1/2} - \tilde{\gamma}j) \quad (21)$$

with

$$C = \frac{4\pi}{3j^3} \left(\frac{\sigma_s}{4\pi}\right)^{3/2} \exp\left(\frac{-4\pi(2K + \bar{K})}{kT}\right) \quad (22a)$$

$$\tilde{\gamma} = \frac{\gamma\sigma_s}{kT}; \quad \tilde{c}_0 = \frac{16\pi Kc_0}{kT} \left(\frac{\sigma_s}{4\pi}\right)^{1/2}; \quad z = \frac{3}{2} - z' \quad (22b)$$

where σ_s is the average area occupied by a surfactant molecule. The droplet radius R_j is defined by

$$\sigma_s j = 4\pi R_j^2 \quad (23)$$

and v_{dj} occurring in Eq. (19) has been replaced by

$$\frac{4}{3} \pi R_j^3 = \frac{4}{3} \pi \left(\frac{\sigma_s j}{4\pi}\right)^{3/2}$$

We need the values of z , \tilde{c}_0 , C , and $\tilde{\gamma}$ for further calculations with the size distribution. The first three quantities should (ultimately) follow from a molecular model (see Sec. VI), but we still need to determine $\tilde{\gamma}$. This quantity plays the role of a Lagrange multiplier coupled to the total interfacial area in the system. Noting that the total number of surfactant molecules in the system is conserved, and assuming that the overwhelming majority of surfactant molecules reside at the droplet interface, we may write

$$c_{sa} = \frac{N_s}{V} = \sum_{j=1}^{\infty} \frac{jn_{dj}}{V} = \sum_{j=1}^{\infty} \frac{j\phi_j}{v_{dj}} \quad (24)$$

with c_{sa} the (known) number density of surfactant molecules in the microemulsion. Equations (24) and (21) together provide a relation for $\tilde{\gamma}$, which adjusts itself automatically to the required value by a slight adaptation of the free surfactant concentration. Note that a second Lagrange multiplier, $\Delta\bar{\mu}$ in Eq. (19) would appear in Eq. (21) if there were no excess phase present in the system. This multiplier couples to the total amount of dispersed volume in the system.

With Eqs. (21)–(24) it is, in principle, possible to obtain measurable properties of saturated droplet-type microemulsions: the total volume fraction of the droplets; the interfacial tension between the microemulsion phase and the excess phase; the average size of the

droplets, i.e., moments of the size distribution; and the polydispersity. In order to obtain numbers one needs to know the values of five independent parameters [see Eqs. (21)–(24)], $(2K + \bar{K})$, Kc_0 , σ_s , l , and z . These values should be obtained from molecular models or from independent experiments. A discussion of possible procedures is presented in the next section.

Before closing this section, we note that in the treatment of droplet-type microemulsions by Borkovec [39] and by Eriksson and Ljunggren [40], fluctuations in the number of molecules inside a droplet as well as fluctuations around the average area occupied by a surfactant molecule are explicitly taken into account. Their treatment leads to a size distribution that can be written in the same form as Eq. (21) but with an additional (weak) dependence of the “constant” C on droplet size. The major effect of treating the fluctuations mentioned above is an effectively different value of z from the one obtained here (but still on the order of 1).

VI. QUANTITIES THAT DETERMINE THE SIZE DISTRIBUTION OF SATURATED DROPLET-TYPE MICROEMULSIONS

A. Bending Elastic Quantities

As mentioned in Sec. III, the effect of an adsorbed surfactant monolayer at the oil/water interface on the bending elastic quantities can be split into two contributions.

1. The contribution of the “brush” formed by the tails of the surfactants (chain contribution)
2. The contribution of the electrical double layer formed by the charged heads of the surfactant molecules, the counterions, and the ions of added salt in the aqueous solution (electrical double layer contribution)

Before presenting results for these quantities, let us first consider how these contributions to the bending elastic quantities can be calculated.

The free energy per unit area of a uniformly bent interface can be written as

$$f_c = f_0 - 2Kc_0(c_1 + c_2) + \frac{1}{2} K(c_1 + c_2)^2 + \bar{K}c_1c_2 \quad (25)$$

where f_0 is the free energy per unit area of flat interface. This equation is not simply F_c/A with F_c given by Eq. (2) but contains a constant contribution f_0 (containing $2Kc_0^2$) from the flat interface. For a sphere, $c_1 = c_2 = 1/R$, and Eq. (25) takes the form

$$f_c = f_0 - \frac{4Kc_0}{R} + \frac{2K + \bar{K}}{R^2} \quad (\text{sphere}) \quad (26)$$

[Note the equivalence of Eqs. (26) and (4) for the interfacial tension, $\sigma(R)$.] For a cylinder, $c_1 = 1/R$ and $c_2 = 0$, so that

$$f_c = f_0 - \frac{2Kc_0}{R} + \frac{K}{2R^2} \quad (\text{cylinder}) \quad (27)$$

If we now compute the free energy of an interface bent into a sphere and that of one bent into a cylinder, we can extract K , \bar{K} , and c_0 by comparing these free energies with the phenomenological expressions Eqs. (26) and (27). Such calculations have been carried out both for the bent brush part of the ionic surfactant monolayer and for the bent electrical double layer part of the adsorbed ionic surfactant monolayer.

Using the analogy that can be drawn between the system of end-grafted polymer chains and the chain part of a surfactant monolayer, Milner and Witten [41] obtained simple analytical expressions for the bending elastic quantities. For the case of a “melt brush,” i.e., one in which the density is forced to be uniform, they obtain

$$K_{\text{ch}} = \frac{3}{2} f_{0,\text{ch}} h_0^2 \quad (28)$$

$$\bar{K}_{\text{ch}} = -\frac{2}{5} f_{0,\text{ch}} h_0^2 \quad (29)$$

$$(Kc_0)_{\text{ch}} = \frac{3}{8} f_{0,\text{ch}} h_0 \quad (30)$$

The subscript ch refers to the chain contribution, and here $f_{0,\text{ch}}$ is the free energy per unit area of a flat brush, for which Milner and Witten obtained the expression

$$f_{0,\text{ch}} = \frac{\pi^2 N \omega^3}{24 \rho_m^2} \left(\frac{3}{\ell^2 C_\infty} \right) kT \quad (31)$$

and $h_0 = N\omega/\rho_m$ is the height of the brush. In the above expressions N is the number of monomers per chain, ω is the number of chains per unit area, ρ_m is the number of monomers per unit volume, ℓ is the bond length, and C_∞ is the characteristic ratio relating the mean square end-to-end distance R_e^2 to the number of monomers per chain and the bond length ($R_e^2 = N\ell^2 C_\infty$ in the melt).

Using typical values for polyethylene chains ($\omega = 4 \text{ nm}^{-2}$, $\rho_m = 34.6 \text{ nm}^{-3}$, $\ell = 0.153 \text{ nm}$, $C_\infty = 6$), one obtains

$$f_{0,\text{ch}} = 0.47 N kT \text{ nm}^{-2} \quad (32)$$

and

$$h_0 = 0.12 N \text{ nm} \quad (33)$$

The method used by Milner and Witten is valid only in the limit of very long hydrocarbon tails on the surfactant molecules. From the calculation presented above it appears that even for relatively short chain surfactants it yields commonly accepted values for the bending elastic quantities, i.e., K , $|\bar{K}|$ are on the order of kT and Kc_0 is on the order of $1kT \text{ nm}^{-1} \cong 10^{-12} \text{ N}$.

Starting from the Poisson–Boltzmann equation it is possible to calculate the free energy of a curved double layer in terms of an expansion in $1/\kappa R$, where κ is the inverse Debye length [$\kappa = (8\pi Q n_{\text{el}})^{1/2}$, with Q defined by Eq. (38) below and n_{el} the number of molecules of 1:1 electrolyte per unit volume] and R is the radius of curvature of the charged interface. Obviously this expansion is valid only for $\kappa R \gg 1$, i.e., for situations where the radius of curvature is (much) larger than the Debye length [28,42–44]. Using this method (the derivations are given in detail in Refs. 43 and 44), one obtains for the electrical

contributions to the bending elastic quantities

$$K_{\text{el}} = \frac{kT}{2\pi Q\kappa} \left(\frac{(q-1)(q+2)}{q(q+1)} \right) \quad (34)$$

$$\bar{K} = \frac{-kT}{\pi Q\kappa} \int_{z=2/(1+q)}^1 \frac{\ln(z) dz}{z-1} \quad (35)$$

$$(Kc_0)_{\text{el}} = \frac{-kT}{2\pi Q} \ln\left(\frac{q+1}{2}\right) \quad (36)$$

where the quantities p and q are related to the surface charge density σ_{el} ,

$$p = 2\pi Q \left| \frac{\sigma_{\text{el}}}{e} \right| \kappa^{-1}; \quad q = (p^2 + 1)^{1/2} \quad (37)$$

where e is the elementary charge and Q is the Bjerrum length,

$$Q = \frac{e^2}{4\pi\epsilon_0\epsilon_r kT} \quad (= 0.7 \text{ nm in water at 298 K}) \quad (38)$$

In this equation, ϵ_r is the dielectric constant of the solution and ϵ_0 is the permittivity of vacuum. The negative sign in $(Kc_0)_{\text{el}}$, Eq. (36), is due to the fact that the electrical double layer tends to bend the interface around the oil side ($c_{0,\text{el}} < 0$).

In writing down Eq. (37) it is assumed that the surface charge density does not depend on curvature. In Ref. 28 arguments are given that the surface charge density does depend on the curvature. There, for an interface bent around the water side, it is assumed that

$$p_{\text{curved}} = p_{\text{flat}} \left(1 + \frac{\xi}{R} \right)^2$$

with ξ between 0.2 and 0.4 nm. Even such small values of ξ have a relatively large influence on the free energy of the bent interface.

It is interesting to consider two limiting cases.

1. Low Surface Charge Densities. In this limit $p \ll 1$, and therefore $q = 1 + p^2/2$. Substituting these results into the expressions above, one obtains

$$K_{\text{el}} = \frac{3\pi kTQ(\sigma_{\text{el}}/e)^2}{2\kappa^3} \quad (39)$$

$$\bar{K}_{\text{el}} = \frac{-\pi kTQ(\sigma_{\text{el}}/e)^2}{\kappa^3} \quad (40)$$

$$(Kc_0)_{\text{el}} = \frac{-kT\pi Q(\sigma_{\text{el}}/e)^2}{2\kappa^2} \quad (41)$$

Interestingly, the form of these expressions is similar to that of the expressions for the bent brush, that is, $f_0 h_0^2$ for K and \bar{K} and $f_0 h_0$ for Kc_0 . Indeed, the free energy per unit area of a flat double layer is, in the limit of small surface charge density, given by

$$f_{0,\text{el}} = \frac{2\pi kTQ(\sigma_{\text{el}}/e)^2}{\kappa} \quad (42)$$

while h_0 can be taken equal to the Debye length κ^{-1} . Using the above results we can write

$$K_{\text{el}} = \frac{3}{4} f_{0,\text{el}} h_0^2 \quad (43)$$

$$\bar{K}_{\text{el}} = -\frac{1}{2} f_{0,\text{el}} h_0^2 \quad (44)$$

$$(Kc_0)_{\text{el}} = -\frac{1}{4} f_{0,\text{el}} h_0 \quad (45)$$

2. High Surface Charge Densities. In this limit, $p = q \gg 1$, and we obtain

$$K_{\text{el}} = \frac{kT}{2\pi Q\kappa} \quad (46)$$

$$\bar{K}_{\text{el}} = \frac{-\pi kT}{6Q\kappa} \quad (47)$$

$$(Kc_0)_{\text{el}} = \frac{-kT}{2\pi Q} \ln\left(\frac{p}{2}\right) \quad (48)$$

Again we find that for typical values of surface charge densities $|\sigma_{\text{el}}/e| \cong 1 \text{ nm}^{-2}$ and for salt concentrations between 0.1 and 0.5 M (of a 1:1 electrolyte), K_{el} and \bar{K}_{el} are on the order of kT , and $|(Kc_0)_{\text{el}}|$ is on the order of 10^{-12} N . Relatively small changes in salt concentration may lead to such a variation in the bending elastic quantities that it induces an inversion of the microemulsion, which, as discussed in Sec. III, is indeed experimentally observed.

Combining, for example, Eq. (30) for the chains [with the numerical values of Eqs. (32) and (33) and choosing $N = 6$ for the chain length] with Eq. (48) for the electrical double layer (with $|\sigma_{\text{el}}/e| = 1 \text{ nm}^{-2}$ and 0.1 M NaCl ($\kappa^{-1} = 1 \text{ nm}$) in the aqueous solution), we find

$$\begin{aligned} Kc_0 &= (Kc_0)_{\text{ch}} + (Kc_0)_{\text{el}} \\ &= \frac{3}{8} f_{0,\text{ch}} h_0 - \frac{kT}{2\pi Q} \ln\left(\frac{p}{2}\right) = (0.76 - 0.18)kT \text{ nm}^{-1} \\ &= 0.58kT \text{ nm}^{-1} = 2.38 \times 10^{-12} \text{ N} \end{aligned}$$

This (a quantity without any subscript symbolizes the total contribution) is of the expected order of magnitude and with a positive sign (i.e., curved as for water droplets in oil). Experiments show [16,28] that for SDS (C_{12} chain) as the surfactant combined with pentanol as the cosurfactant (20% w/w in cyclohexane), c_0 is zero at 0.15 M NaCl, and thus at 0.1 M NaCl the system forms an O/W microemulsion with Kc_0 negative.

The choice of $N = 6$ in the above numerical example is reasonable for comparison with the experiments, since according to Ref. 41 a mixture in the interface of about 25% C_{12} chains and 75% C_5 chains behaves in the bending as if all the chains had a length somewhat greater than C_5 , the extra length of the C_{12} chains sticking out of the closely packed C_5 layer offering very little resistance to bending.

Our conclusion is that the theory, as described above, fits reasonably well to experiments, although the contribution of the chains to Kc_0 may be somewhat too large and/or the double layer contribution somewhat too small. The double layer contribution would become larger if we were to take account that the surface charge density increases on bending around the water side (see Ref. 28), and the chain contribution may have been overvalued by applying a theory developed for long chains (see Ref. 41) to rather short chains.

In general it seems a good idea to check theories at the condition where c_0 becomes zero and to remember that at the present stage the theories, both for the electrical effects and for the chains, may need quantitative adaptations on the order of several tens of percent.

Experimentally, the bending elastic modulus K as measured by ellipsometry is indeed found to be on the order of $(0.1-1)kT$ for quite a wide range of microemulsion systems; see, e.g., Ref. 45 for a system with a single-chain ionic surfactant plus cosurfactant, Ref. 46 for a system with a double-chain ionic surfactant in which the chain length of the oil (linear alkane) is varied, and Ref. 47 for a system with a nonionic surfactant in which the chain length of the surfactant is varied.

In ellipsometry the fluctuations in the interface position (capillary waves) manifest themselves, and when the interfacial tension γ is sufficiently small, the influence of K on the interfacial waves can be measured.

As follows easily from Eq. (3) for the bending free energy of a single drop, the term with the Gaussian modulus is proportional to the number of droplets in a system, just as the mixing entropy is. For this reason, the Gaussian modulus can be obtained from experiments only by using an expression for the mixing entropy. Several assumptions in the literature [27,48-52] point to values roughly in between $-kT$ and $+kT$ for \bar{K} .

Just like the Gaussian bending elastic modulus, the quantity Kc_0 can, in general, be obtained only by assuming a model for the mixing entropy. However, one of us [53] showed recently that when the average size of the droplets is large (say, several tens of nanometers), the quantity Kc_0 can, to a good approximation, be obtained from an average radius and the interfacial tension γ between the microemulsion phase and the excess phase without the need for numerical values of $(2K + \bar{K})$, σ_s , l , and z (see Sec. V, just before the last paragraph) via

$$\gamma = 2Kc_0/R_{ik}^{1/(i-k)} \quad (\text{large droplets}) \quad (49)$$

In this equation, the average droplet radius is effectively a ratio of moments of the size distribution, Eq. (21), i.e.,

$$\begin{aligned} R_{ik} &= \frac{\langle R^i \rangle}{\langle R^k \rangle} = \frac{\sum_{j=1}^{\infty} R_j^i \rho_j}{\sum_{j=1}^{\infty} R_j^k \rho_j} = \frac{\sum_{j=1}^{\infty} R_j^i [\phi_j / (4/3)\pi R_j^3]}{\sum_{j=1}^{\infty} R_j^k [\phi_j / (4/3)\pi R_j^3]} \\ &= \frac{\sum_{j=1}^{\infty} R_j^i j^{z-3/2} \exp(-\tilde{\gamma}j + \tilde{c}_0 j^{1/2})}{\sum_{j=1}^{\infty} R_j^k j^{z-3/2} \exp(-\tilde{\gamma}j + \tilde{c}_0 j^{1/2})} \end{aligned} \quad (50)$$

where R_j is defined by Eq. (23). Equation (49) can be obtained from Eq. (50) by replacing the summations by integrations and assuming that $\tilde{c}_0 \gg \tilde{\gamma}$. This derivation is given in some detail in Ref. 53. Note, however, that in this reference a slightly different definition of R_{ik} was used. i and k depend on the technique used to measure the droplet size; e.g., if the volume of the dispersed phase is measured and the interfacial area is known, one obtains R_{ik} with $i = 3$, $k = 2$, whereas by measuring the radius of gyration one has approximately $i = 8$, $k = 6$. Equation (49) is a generalization (to polydisperse systems) of the result of de Gennes and Taupin [18] using ideas from Robbins [11] for strictly monodisperse systems. We emphasize that, strictly speaking, Eq. (49) has only limited applicability, i.e., its right-hand side is the first term in a series in $1/R_{ik}^{1/(i-k)}$ of which convergence is questionable in situations where the average size of the droplets is smaller than about 10 nm. Once Eq. (49) is valid, however—that is, at large average radius and therefore at small γ —the quantity Kc_0 can be obtained *directly* from experiments without making assumptions for the mixing entropy and the value of z .

Incidentally, for the interfacial tension γ^* and the radius R^* , belonging to the maximum volume fraction ϕ_j (this R^* must be close to the average radius $R_{ik}^{1/(i-k)}$), an equation similar to Eq. (49) can be derived very simply from $\partial\phi_j/\partial j = 0$ [see Eqs. (21)–(24)]. This leads exactly to

$$\gamma^* = \frac{2Kc_0}{R^*} + \frac{zkT}{4\pi(R^*)^2} \quad (51)$$

The second term on the right in Eq. (51) is on the order of 10% of the first term.

In the next section we consider experimentally obtained data sets from which Kc_0 is extracted in the way described above. These results confirm the expectation that the spontaneous curvature, c_0 , is on the order of the inverse average droplet radius in a saturated microemulsion system. This expectation follows from the relation, Eq. (5), between c_0 and R_{MIN} and the fact that the entropy of mixing makes the average droplet radii somewhat smaller than R_{MIN} .

B. Molecular Area of Surfactant(s)

The average area occupied by a surfactant molecule, σ_s , is obtained by measuring the tension of a macroscopic oil/water interface as a function of the surfactant concentration below the cmc and applying the Gibbs adsorption equation. This area turns out to be fairly independent of the concentrations of the constituent parts of a given microemulsion (i.e., salt and/or cosurfactant concentration) [5,54]. It varies between approximately 0.6 nm^2 for AOT systems [54] and about 1 nm^2 for SDS–cosurfactant (linear alcohol) systems [5]. In the latter situation, this area is shared with approximately two to three cosurfactant molecules. It is assumed here that the area per surfactant molecule at the droplet interface does not differ from the one at the macroscopic oil/water interface [see, however, the discussion following Eq. (38)]. The only experimental indication that we are aware of that indeed points to the validity of this assumption comes from small-angle X-ray scattering (SAXS) measurements [55].

C. Length Scale for Configurational Entropy

As already indicated, the length l cannot be measured directly. It is sensitive to the model employed in the description of a microemulsion. For the phenomenological model as described in this chapter, it is found to be on the order of the cube root of a molecular volume in the liquid state [31], that is, approximately 0.5 nm.

D. Value of z

In Ref. 27, Kegel and Reiss estimated z of the basis of experiments on microemulsions. Assuming that the average radius of a drop never exceeds $2/c_0$, they found the inequality (independent of their somewhat different definition of R_{ik})

$$3/4 < z < 3/2 \quad (52)$$

VII. GENERAL PROPERTIES OF THE SIZE DISTRIBUTION AND EXPERIMENTAL TEST OF THE THEORY

A. Order of Magnitude of Measurable Properties of Saturated Droplet-Type Microemulsions

We summarize the estimated ranges of the quantities discussed in the previous section:

$$0 < (2K + \bar{K})/kT < 3 \quad (53a)$$

$$0.01 < |Kc_0|/(kT \text{ nm}^{-1}) < 1 \quad (53b)$$

$$0.5 < \sigma_s \text{ nm}^{-2} < 1 \quad (53c)$$

$$l^3 \approx 0.1 \text{ nm}^3 \quad (53d)$$

$$3/4 < z < 3/2 \quad (53e)$$

As mentioned in the discussion around Eqs. (21)–(24), we need values of the five parameters listed in Eqs. (53) and of the surfactant concentration, c_{sa} , to be able to calculate values of various properties of microemulsions (O/W + O or W/O + W). Of these five parameters the area per surfactant molecule, σ_s , can be determined accurately from the Gibbs adsorption equation, Eq. (1), and there is only a small uncertainty regarding the values of l and z .

We therefore choose $\sigma_s = 1 \text{ nm}^2$ in the following calculations and take $l^3 = 0.1 \text{ nm}^3$ and $z = 3/2$ or $3/4$. We choose 10 mM for the surfactant concentration in Table 1 (and 50, 16.7, and 8.3 mM, respectively, in Fig. 5), assuming that all of it is adsorbed and the amount of dissolved surfactant is negligible. A number of values of $2K + \bar{K}$ and of Kc_0 are taken within the ranges indicated in Eqs. (53a) and (53b).

Then we (iteratively) calculate γ from Eqs. (21)–(24). This results in the size distribution $\{\phi_j\}$, from which the average size of the droplets follows using Eq. (50) and the total volume fraction of the droplets, ϕ , by summing Eq. (21) over all categories. In Fig. 5 we show a set of typical size distributions obtained in this way.

Table 1 Properties of the Size Distribution as a Function of the Input Parameters Kc_0 and $2K + \bar{K}$ ^a

| Kc_0 ($kT \text{ nm}^{-1}$) | $2K + \bar{K}$ (kT) | γ ($kT \text{ nm}^{-2}$) | R_{32} (nm) | ϕ | ε |
|---------------------------------|-------------------------|-----------------------------------|---------------|--------|---------------|
| 0.01 | 1 | 0.1 | 1.3 | 0.0028 | 0.46 |
| | 2 | 0.0021 | 14.0 | 0.03 | 0.34 |
| | 3 | 0.00048 | 47.1 | 0.12 | 0.20 |
| 0.1 | 1 | 0.43 | 0.8 | 0.0017 | 0.36 |
| | 2 | 0.065 | 3.6 | 0.0072 | 0.23 |
| | 3 | 0.0285 | 7.6 | 0.0172 | 0.16 |
| 0.5 | 1 | >2 | <1 | — | — |
| | 2 | 1.0 | 1.1 | 0.0023 | 0.19 |
| | 3 | 0.545 | 2.0 | 0.004 | 0.14 |
| 1 | 1 | >2 | <1 | — | — |
| | 2 | >2 | <1 | — | — |
| | 3 | 1.97 | 1.1 | 0.0028 | 0.14 |

^a The values of the other parameters were fixed at $c_{sa} = 10 \text{ mM}$, $l^3 = 0.1 \text{ nm}^3$, $z = 3/2$, $\sigma_s = 1 \text{ nm}^2$. “Droplets” are considered to be of molecular size if $R_{32} < 1 \text{ nm}$ and $\gamma > 2kT \text{ nm}^{-2}$.

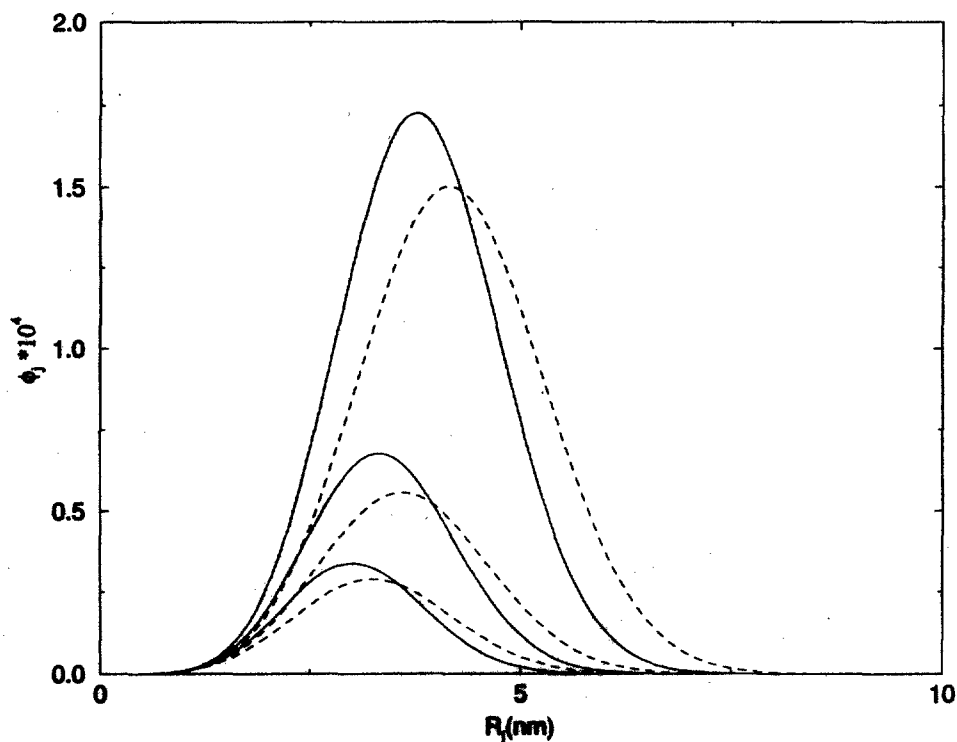


Figure 5 Size distributions calculated for $Kc_0 = 0.05kT \text{ nm}^{-1}$. The solid curves were calculated using $z = 3/2$; for the dashed ones, $z = 1$ was used. Going from the upper to the lower curves, the surfactant concentration was fixed at 50, 16.7, and 8.3 mM, respectively. The values of the other parameters are $l^3 = 0.1 \text{ nm}^3$, $\sigma_s = 1 \text{ nm}^2$, $2K + \bar{K} = 3kT/2$. (From Ref. 27)

The polydispersity ε is obtained via

$$\varepsilon = \left(\frac{\langle R^2 \rangle}{\langle R \rangle^2} - 1 \right)^{1/2} \quad (54)$$

From experimental investigations reported in the literature in which the interfacial tension, the average droplet size, and/or the polydispersity of Winsor II systems is measured (see, e.g., Refs. 28, 46–48, 50, and 54–56), we estimate that at $c_{sa} \approx 10 \text{ mM}$ the average size of the droplets is in the range $R_{32} = 2\text{--}20 \text{ nm}$, the macroscopic interfacial tension $\gamma = 0.001\text{--}0.1 \text{ mN/m}$, the volume fraction of the droplets $\phi \approx 0.01\text{--}0.1$, and the polydispersity is roughly $0.1 \leq \varepsilon \leq 0.4$. We raise the question of whether the orders of magnitude of this set of data can be reproduced by the theory using the values of the parameters in the ranges given in Eqs. (53).

Using the values of the parameters as mentioned above, it is found that the combination $2K + \bar{K}$ should be larger than zero in order for a microemulsion with average droplet size on the order of 1 nm (and interfacial tension smaller than order $kT \text{ nm}^{-2}$) to be stable. The results are summarized in Table 1.

First of all we can check that except for the upper two rows in Table 1, Eq. (49) describes the relation between γ , Kc_0 , and R_{32} surprisingly well, even for very small R_{32} . It follows from Table 1 that when Kc_0 is increased, $2K + \bar{K}$ should be increasingly larger in order

for drops of average sizes greater than 1 nm to be stable. If the value of z is set equal to $3/4$, a larger average drop size is found (approximately 10–20% larger for the relevant values of the other parameters) as well as a slightly smaller polydispersity (not shown in Table 1). Generally, with the values of the parameters in the ranges given in Eqs. (53), the average droplet size varies from molecular lengths to approximately 50 nm, the volume fraction from about 0.002 to about 0.12, the interfacial tension from about 0.002 to 8 mN/m (at $T = 298$ K), and the polydispersity from approximately 14% to 46%.

We conclude from this section that values of the parameters indicated in Eqs. (53) estimated from experiments give predictions of measurable properties of droplet-type microemulsions that are of the same order of magnitude as those found in experiments. No additional concepts are required to force this agreement.

B. Quantitative Comparison with Experiments

In this section, measured average droplet sizes, droplet volume fractions, and interfacial tensions are compared with the thermodynamic formalism as presented in Sec. V. These quantities can be calculated by fixing values of l , z , σ_s , Kc_0 , and $2K + \bar{K}$, numerically solving Eq. (24) with Eqs. (21)–(23) for $\tilde{\gamma}$ (with fixed c_{sa}), and subsequently calculating the average size of the droplets by using Eq. (50). In practice, not all values of these quantities are known. For l , z , and σ_s , one can make reasonable estimates, but in order to obtain the bending elastic quantities Kc_0 and $2K + \bar{K}$, one needs, at the current state of the art, input from independent experiments. At the moment there are no microemulsion systems for which both Kc_0 and $2K + \bar{K}$ are known without some theory (of droplet-type microemulsions) being used. Therefore the whole calculation as outlined above should be done iteratively, using trial values of one or more of the bending elastic quantities and varying them (within certain windows) until convergence is reached between theory and at least one measured quantity. It is therefore convenient to simplify the equations that interrelate these quantities. By replacing the summations by integrations in Eq. (50), substituting $x = j^{1/2}$, and using the method of steepest descent, the average radius can be approximated as (see Refs. 27 and 53 for details)

$$R_{ik} = \left(\frac{\sigma_s}{4\pi} \right)^{(i-k)/2} \exp[f(x_i^*) - f(x_k^*)] \quad (55)$$

and the total volume fraction of the droplets may be written as

$$\phi = 2C \left(\frac{\pi}{\tilde{\gamma}} \right)^{1/2} e^{f(x_3^*)} \quad (56)$$

with

$$f(x_i^*) = -\tilde{\gamma}(x_i^*)^2 + \tilde{c}_0 x_i^* + [2(z-1) + i] \ln(x_i^*) \quad (57)$$

and

$$x_i^* = \frac{\tilde{c}_0 + \{\tilde{c}_0^2 + 8[2(z-1) + i]\tilde{\gamma}\}^{1/2}}{4\tilde{\gamma}} \quad (58)$$

x_i^* is the maximum of the function $x^{2(z-1)+i} \exp(-\tilde{\gamma}x^2 + \tilde{c}_0x) = \exp\{-\tilde{\gamma}x^2 + \tilde{c}_0x + [2(z-1) + i] \ln x\}$. The subscript i of x_i^* refers to the value of i in Eqs. (57) and (58). Note that these expressions differ from the ones given in Refs. 27 and 53 owing to the slightly different definition of R_{ik} used in this work. Equation (58) is [by the definitions given in

Eqs. (22) and (23)] analogous to Eq. (51). Now the measurable properties of interest in saturated droplet-type microemulsions can be calculated without having to perform extensive computations.

1. Average Droplet Size and Macroscopic Interfacial Tension as a Function of Droplet Volume Fraction

As far as we are aware, the only system for which the volume fraction of the droplets, the average radius (R_{32}), and the tension of the macroscopic oil/water interface have been measured is a Winsor II system composed of SDS, pentanol, cyclohexane, and 0.2 M NaCl with equal volumes of water and oil phases. This system was studied in Ref. 55. The bending elastic modulus of this system was measured by ellipsometry [50]. The results of Sec. V imply that when l and z are fixed, there are still two unknown parameters: the Gaussian bending elastic modulus and the preferred curvature. Therefore, we choose to test the theory on consistency, that is, we fix z and l and fit the (R_{32}, ϕ) data with Eqs. (55)–(58)—we choose Kc_0 and $2K + \bar{K}$, determine the values of $\tilde{\gamma}$ that generate the experimental values of ϕ , and compare the calculated droplet radii with the experimental ones. This procedure is iterated until maximum agreement with the experimental droplet radii is obtained. Subsequently, we compare the values of the interfacial tension γ from $\tilde{\gamma}$ [Eq. (22)] that were necessary to generate these (R_{32}, ϕ) data with the experimentally measured values. Note that in this treatment the volume fraction of the droplets rather than the surfactant concentration conveniently determines the Lagrange multiplier $\tilde{\gamma}$. We emphasize that the last mentioned comparison requires no adjustable parameters. Figure 6a shows the experimentally determined (R_{32}, ϕ) data together with the best fit results for constant $z = 3/2$ and c_0 and different values of \bar{K} . Figure 6b shows the set of values of the interfacial tension that were used to generate these data, again together with the experimental results from Ref. 55.

We note, as already mentioned, that the definition of R_{ik} that was used in Ref. 27 is different from the definition given in Eq. (50); that is, in Ref. 27 a volume fraction averaged radius was calculated instead of the number density averaged radius, Eq. (50). For this reason the values of Kc_0 and $2K + \bar{K}$ are slightly different from the ones found in Ref. 27.

Looking at Fig. 6, we note that the agreement is excellent. Comparable agreement is found over the whole range of z as given by Eq. (53e). The value of c_0 obtained in this way increases somewhat with decreasing z , whereas the value of \bar{K} decreases and even becomes negative. This analysis proves that the theory is consistent for this aspect; i.e., fitting the theory to experimentally obtained (R_{32}, ϕ) data generates the variation of interfacial tension with volume fraction of the droplets without any additional adjustable parameters.

The value of c_0 can also be obtained independently from the work reported in Ref. 28. In this work, among other things, the droplet radii and the interfacial tensions as a function of the cosurfactant concentration for the same system as used in Ref. 55 were measured. For the system containing 19% pentanol, which is closest to the 20% used by van Aken [55], we estimate $\gamma = 0.02 \text{ mN/m} = 0.00487kT \text{ nm}^{-2}$, and $R_{32} = 12 \text{ nm}$. Substituting these values into Eq. (49) and using the fact that $K = 1kT$ for this system, we obtain $c_0 = 0.029kT \text{ nm}^{-1}$, which is remarkably close to the value of $0.035kT \text{ nm}^{-1}$ used in Fig. 6. (Moreover, it is expected that c_0 indeed increases with increasing cosurfactant concentration.)

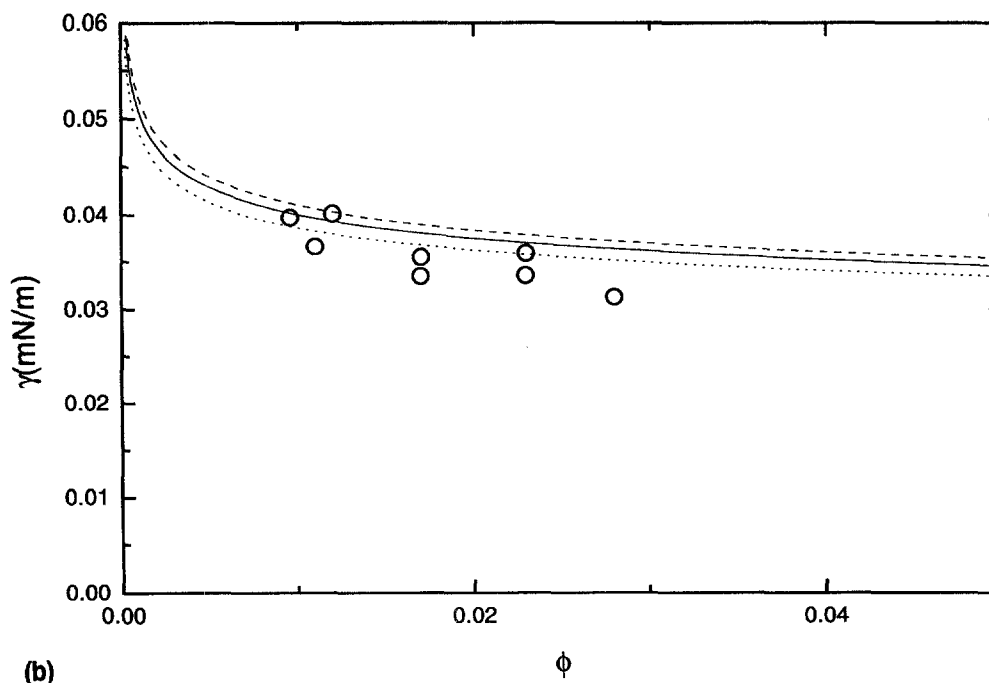
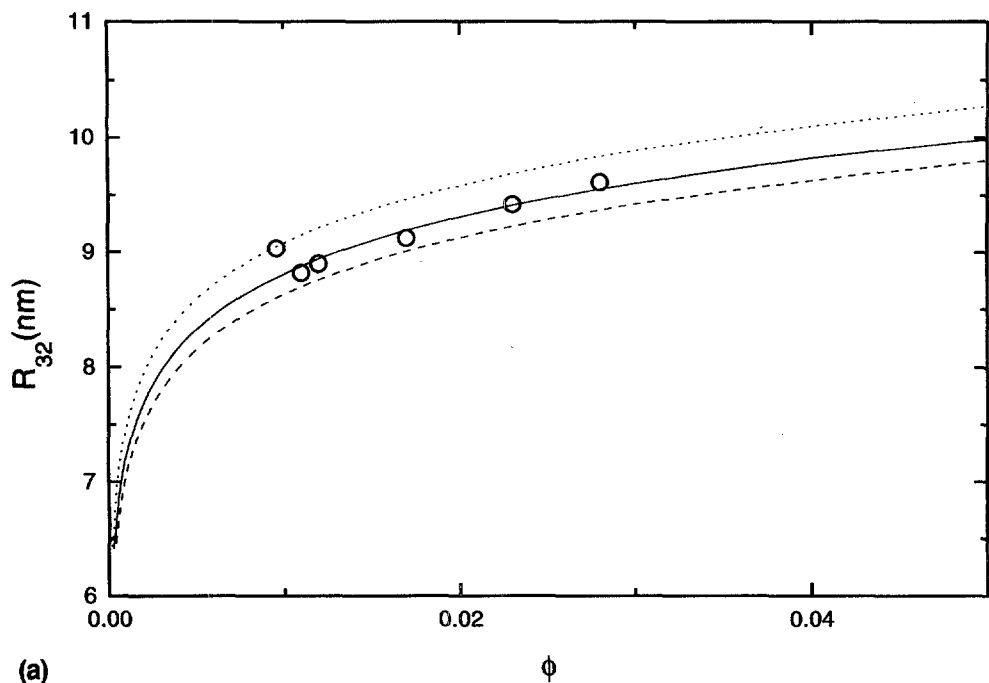


Figure 6 Experimental data of van Aken [55], experimental droplet radius R_{32} versus volume fraction ϕ of the droplets together with theoretical lines calculated from Eqs. (55)–(58) using $K = kT$ [50], $l^3 = 0.1 \text{ nm}^3$, $\sigma_s = 1 \text{ nm}^2$, $z = 3/2$, $c_0 = 0.035 \text{ nm}^{-1}$, and $\bar{K}/kT = 0.25$ (dotted line), 0.22 (solid line), and 0.20 (dashed line). In (a) data were fitted using c_0 and \bar{K} as free parameters. In (b) the variation of the interfacial tension γ necessary to produce the lines in (a) are plotted together with the experimental points. There is no additional free parameter.

2. Macroscopic Interfacial Tension and Average Droplet Sizes as a Function of Salt Concentration

In Sec. VI expressions were given for the chain contributions and the electrical double layer contributions to the bending elastic quantities. There it was argued that the theoretical results fit reasonably well to experiments but not well enough to give accurate values for all parameters involved.

With this in mind, we start by writing the preferred curvature as

$$c_0 = \frac{(c_0 K)_{\text{ch}} + (c_0 K)_{\text{el}}}{K} \quad (59)$$

where the subscript ch again refers to the contribution of the surfactant chains. The electrical part of the preferred curvature is given by Eq. (36). The chain contribution can in principle be obtained from Eq. (59) if the salt concentration at which $c_0 = 0$ (or, of course, any other known value) is known. We prefer this approach rather than using an estimate for the chain contribution based on Eq. (30) as suggested earlier following Eq. (48).

In Ref. 46, interfacial tension was measured as a function of the salt concentration for systems composed of AOT, brine, and linear alkanes of varying chain length (C_8 , C_{10} , C_{12} , C_{14}). In this work, the bending elastic moduli of these systems were determined by ellipsometry. The droplet radii of these systems are reported elsewhere [48]. The interfacial tension as reported in Ref. 46 first decreases, goes through a minimum, and subsequently increases with increasing salt concentration. The minimum (and its immediate neighborhood) corresponds to an (actually quite special kind of) Winsor III system: a microemulsion phase coexisting with excess oil and brine. The preferred curvature should be zero at this interfacial tension minimum. Therefore we obtain $(c_0 K)_{\text{ch}} = -(c_0 K)_{\text{el}}$ at the salt concentration at which the interfacial tension is at a maximum. Note that in the Winsor III region we are not dealing with droplets but (most probably) with a structure with zero mean curvature. In that case we expect, contrary to the situation with droplets discussed in Sec. III [see in particular Eq. (5)], that the interfacial tension is at a minimum when $c_0 = 0$. Very similar ideas were used in Ref. 28 to give a quantitative explanation of the interfacial tension γ and the droplet radius R as a function of the salt concentration on W/O + W microemulsions stabilized with SDS and pentanol.

The constant value of the chain contribution may be considered as a zeroth-order approximation, where it is assumed that the density of the chains is independent of the salt concentration. A motivation for this assumption is that the molecular area of the surfactant as a function of salt concentration in the systems used in Ref. 46 was found [54] to be constant within the range of experimental error.

The interfacial tension was calculated from surfactant conservation by simplifying Eq. (24) in the same way as the expressions for the volume fraction and average radii were simplified by Eqs. (55)–(58). This expression reads

$$c_{sa} = 2 \left(\frac{\pi}{\bar{\gamma}} \right)^{1/2} l^{-3} \exp \left(\frac{-4\pi(2K + \bar{K})}{kT} \right) e^{f(x_2^*)} \quad (60)$$

with, from Eqs. (57) and (58),

$$f(x_2^*) = -\tilde{\gamma} x_2^{*2} + \tilde{c}_0 x_2^* + 2z \ln(x_2^*) \quad (61a)$$

where

$$x_2^* = \frac{\tilde{c}_0 + (\tilde{c}_0^2 + 16z\tilde{\gamma})^{1/2}}{4\tilde{\gamma}} \quad (61b)$$

It can be seen from Eqs. (60) and (61) that when K , c_{sa} , and Kc_0 are known and z and l are fixed, the interfacial tension still depends on a single variable, the Gaussian bending elastic modulus. The results together with the experimental data are shown in Fig. 7. The fixed independent parameters that were used to calculate these curves are listed in Table 2. Due to the fact that in Ref. 27 an erroneous expression for $(Kc_0)_{el}$ was used, the values of $(Kc_0)_{ch}$ in Table 2 are different from the ones used in Ref. 27. We note that the values of $(Kc_0)_{ch}$ listed in Table 2 are indeed of the same order of magnitude as the ones predicted by Eqs. (28)–(31) for polyethylene chains (with small N , say $N < 10$). The decrease in $(Kc_0)_{ch}$ with increasing chain length of the oil may be understood qualitatively as follows. Assuming that in going from C_8 to C_{12} , fewer and fewer oil molecules penetrate into the surfactant brush (and there are indeed strong experimental indications pointing to the validity of this approach; see Ref. 57), then effectively the number of monomers per unit volume, ρ_m , decreases and therefore, from Eqs. (28)–(31), $(Kc_0)_{ch}$ decreases.

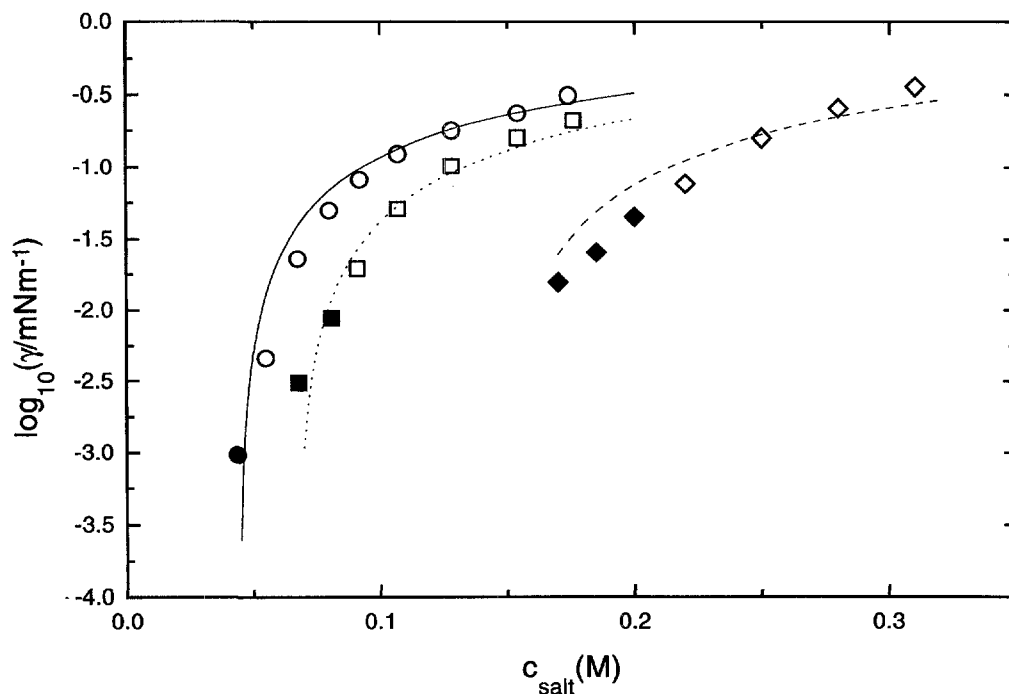


Figure 7 Interfacial tension of the planar interface between the microemulsion and the excess phase as a function of the salt concentration for systems composed of AOT (sodium diethylhexylsulfosuccinate), brine, and linear alkanes of varying chain length. Points are experimental data obtained for C_8 (\circ , \bullet), C_{10} (\square , \blacksquare), and C_{12} (\diamond , \blacklozenge) linear alkanes making up the oil phase. Open symbols refer to Winsor II systems; corresponding filled symbols indicate the Winsor III region where the theory is no longer valid. The lines were calculated according to Eqs. (60) and (61), the fixed parameters listed in Table 2, and suitably chosen values of $\bar{K}/kT = 0.8$ (C_8 systems), 0.39 (C_{10} systems), and 1.2 (C_{12} systems). (Experimental data from Ref. 46.)

The theoretical lines in Fig. 7 correspond to suitably chosen values of the Gaussian bending elastic modulus \bar{K} . Other values of this parameter only translate the curves through the $(\gamma, c_{\text{salt}})$ plane without altering their shapes. It should be emphasized that the curves are all unique; that is, there are no values of \bar{K} that allow the C_{10} or C_{12} data to be described by the parameters corresponding to the C_8 data. It is clear from Fig. 7 that the relevant experimental data (i.e., the ones corresponding to Winsor II systems) are described rather well by the theory. Even the agreement with the C_{12} data is reasonable, which is somewhat unexpected because of the small value of K for this system ($0.15kT$). For these small values of K , the *Ansatz* for the interfacial tension, $\sigma(R_j)$, Eq. (20) (i.e., up to second order in the inverse droplet radius), is no longer believed to be a good approximation.

Now, using the parameters listed in Table 2 and the values of \bar{K} that were used to calculate the theoretical lines in Fig. 7, the droplet radii were calculated by using Eq. (55) with $i = 3$, $k = 2$. The results are shown in Fig. 8, together with the experimentally determined radii reported in Ref. 48. It is emphasized that the theoretical lines in Fig. 8

Table 2 Fixed Parameters Used to Calculate the Dependence of Interfacial Tension on Salt Concentration^a

| System (oil phase) | K (kT) | $(Kc_0)_{\text{ch}}$ ($kT \text{ nm}^{-1}$) | σ_s (nm^2) |
|-----------------------|--------------|---|------------------------------|
| Octane (C_8) | 0.85 | 0.365 | 0.71 |
| Decane (C_{10}) | 0.95 | 0.334 | 0.67 |
| Dodecane (C_{12}) | 0.15 | 0.255 | 0.64 |

^a A surfactant concentration of 10 mM in the microemulsion phase was used in all cases.
Source: Refs. 46 and 54.

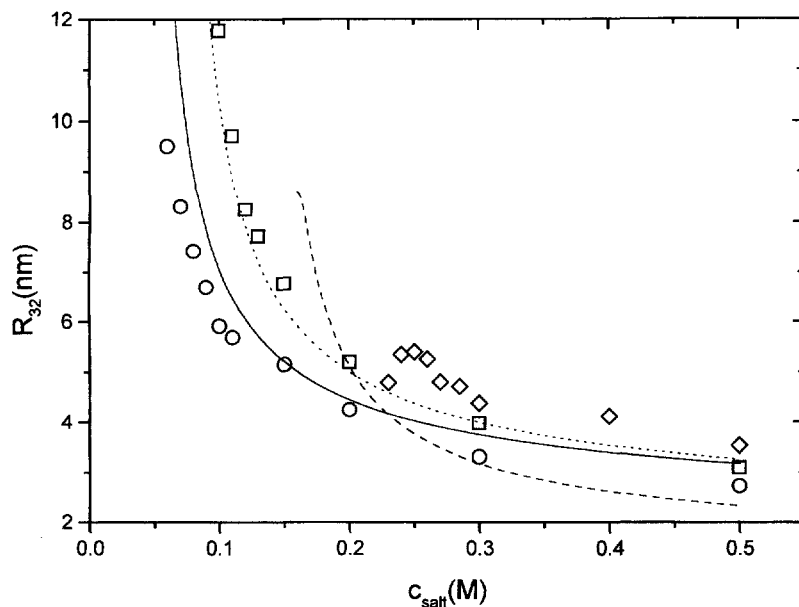


Figure 8 Variation of average droplet radius (R_{32}) as a function of salt concentration for the same systems as in Fig. 7. Theoretical lines were calculated using Eqs. (60) and (61) with Eq. (55) using the same parameters as in Fig. 7. The surfactant concentration was fixed at $c_{sa} = 60$ mM, as in Ref. 48. (Experimental points from Ref. 48.)

are calculated without any adjustable parameters.

As can be seen from Fig. 8, the agreement between theory and experiments is excellent for the C_{10} systems and quite good for the C_8 systems, although in the latter case it seems as if the difference between theory and experiments is a systematic shift parallel to the salt concentration axis. A possible explanation is that different batches of AOT might have been used in the work reported in Refs. 46 and 48. Very small amounts of adsorbed contaminants and/or hydrolysis products are expected to have a significant influence on (the chain contribution to) the preferred curvature. Indeed, if a slightly larger value of $(Kc_0)_{\text{ch}}$ than the one listed in Table 2 is used for the C_8 systems (i.e., $0.380kT \text{ nm}^{-1}$ instead of $0.365kT \text{ nm}^{-1}$), then excellent agreement is observed between theoretical and experimental droplet radii as a function of salt concentration. Clearly the theory predicts values of the radii that are too small in the case of the C_{12} system.

We note that for the AOT systems the values of the Gaussian bending elastic moduli are found to be significantly greater than the one that was found for the SDS plus pentanol system (see Sec. VII.B.1). This difference might be due to the difference in molecular geometry between AOT and SDS/pentanol. We feel that more experimental work on other systems should be done and that sophisticated models for surfactant monolayers at oil/brine interfaces should be developed in order to be able to gain some understanding of this peculiar behavior of the Gaussian bending elastic modulus.

VIII. CONCLUDING REMARKS

A. What Can Be Understood?

The concept of a competing droplet size-dependent interfacial tension and entropy of mixing gives a good qualitative understanding of the behavior of saturated droplet-type microemulsions (variation of average droplet size and interfacial tension with salt concentration). As, at a certain point, the preferred curvature changes sign, an inversion from an O/W to a W/O system is found as well.

Quantitatively the thermodynamic formalism as worked out in Sec. V leads to good agreement with experiments. In Sec. VII.B.1 it was shown that the variation of average droplet radius with the volume fraction of the droplets can be described quantitatively by the theory presented in Sec. V using the same set of “adjustable” parameters [Kc_0 and $(2K + \bar{K})$] that quantitatively describes the variation of the interfacial tension γ with droplet volume fraction. The value of Kc_0 that has been used to describe these data could also be verified, at least approximately, with an independent experiment using Eq. (49).

There is still good agreement between theory and experiment even when all but one parameter are fixed (Sec. VII.B.2). In that comparison, a molecular model for the variation of the preferred curvature with salt concentration was used. It was shown that the variation in the interfacial tension γ with salt concentration can be described well by the theory using the Gaussian bending elastic modulus as a free parameter. Using the same values of the Gaussian bending elastic modulus and keeping all other parameters fixed, the variation of average droplet radius with salt concentration is also described quite well by the theory.

Interestingly, both in Sec. VII.B.1, where a system composed of SDS, pentanol, cyclohexane, and water plus salt was compared to the theory, and in Sec. VII.B.2, where a system containing AOT, water plus salt, and linear alkanes of different chain lengths was evaluated, the Gaussian bending elastic modulus was found to be greater than zero. Although in the first situation this positive sign is hardly significant (due to the experimental

error in K of at least 10%), it definitely is in the second situation. This positive sign is not to be expected for surfactant monolayers. We believe that this observation is a challenging motive for further experimental work on droplet-type microemulsions and theoretical work on surfactant monolayers at oil/water interfaces.

B. What Is Not Understood or Is Only Partly Understood?

A theory that predicts both global phase behavior and detailed properties of the phases as a function of experimentally adjustable quantities without any adjustable parameters still seems far away. Below we list a number of, in our opinion, important problems that need to be solved in order to be able to proceed further.

First of all, there still are a few subtleties in the theory of droplet-type microemulsions:

1. As discussed in Sec. VI following Eq. (38), it is to be expected that the surface charge density at the droplet interface depends on curvature owing to the fact that the Gibbs surface does not necessarily coincide with the surface of closest packing of the surfactant molecules. Indeed, strong indications for this effect were found [28] for systems with SDS as a surfactant and pentanol as a cosurfactant. However, for the AOT systems analyzed in Sec. VII.B.2, it was not necessary to invoke such an effect. We conclude, therefore, that the magnitude of this effect [that is, the value of ξ as defined following Eq. (38)] depends on the type (geometry) of surfactant being used and is (to a good approximation) absent from the type of AOT systems studied in Sec. VII.B.2. This suggests another challenging issue in a theoretical treatment of surfactant monolayers at oil/water interfaces, in addition to the relation between the type (geometry) of surfactant and the value of \bar{K} as discussed above and at the end of Sec. VII.B.2.
2. A consistent treatment of finite size effects and fluctuations of the volume of the droplets (beyond capillary waves) is needed. Ideally such a theory should come up with a value of z' . In the comparison between theory and experiments (see Sec. VII), we find no indications for a value of z' being different from 0.

C. Questions Regarding Non-Droplet Phases

The emphasis in this work was on droplet-type microemulsions. As promised in Sec. IV, we now present a short discussion on non-droplet phases.

At the end of Sec. III we mentioned that at zero preferred curvature and low surfactant concentrations, a system consisting of a surfactant-rich middle phase coexisting with excess oil and water phases (Winsor III) is found. If the preferred curvature is altered (by temperature, salt, or cosurfactant), a continuous transition to a droplet-type microemulsion coexisting with an excess phase is observed.

If more and more surfactant is added to a Winsor III system, the surfactant-rich phase swells at the expense of the excess oil and water phases. From a certain point, a single surfactant-rich phase is found. Upon increasing the amount of surfactant even further, a first-order transition to a lamellar phase may be observed. In a special case, it has been shown that the coexistence region between the (bicontinuous) microemulsion phase and a lamellar phase was extended into the region where the surfactant-rich phase coexists with excess oil and water, leading to a four-phase equilibrium: water–lamellar phase–microemulsion phase–oil [58]. In Ref. 46, even a three-phase equilibrium, water–lamellar phase–oil, was observed, the bicontinuous microemulsion phase apparently being absent.

In order to be able to extend the approach described in this contribution beyond microemulsions with a droplet structure, the (in our opinion) most important question to be resolved is: What is the structure of the middle-phase microemulsion, and how does it contribute to the mixing entropy of the system? An answer to this question may also provide a (qualitative) explanation regarding the limited swellability of a middle-phase microemulsion, that is, the observation that the surfactant-rich phase remains in between excess oil and water in spite of the fact that the middle phase is probably bicontinuous.

Strey and coworkers [59] showed evidence that the structure of such a middle phase in a nonionic surfactant system resembles a “molten cubic” structure. This is a multiply connected structure, and this may indeed provide an answer to the question as to why a middle phase does not swell. It is not clear yet whether this structure is the same for all middle-phase microemulsions.

In a rather successful phenomenological (lattice) theory put forward by Andelman and coworkers [20], the middle-phase microemulsion is regarded as an ensemble of noninteracting monolayers. These monolayers are characterized by their persistence length [18], which in turn depends exponentially on the bending elastic modulus (in contrast to polymers, where this dependence is linear). The collective character of a middle-phase microemulsion is then taken into account by invoking an “entropy of mixing” comparable to the Bragg–Williams approach in Ising models, also referred to as “random mixing” (i.e., the probabilities of neighboring lattice sites containing water or oil are uncorrelated). As a result, the characteristic length in the system (the so-called dispersion size) is predicted to be somewhat smaller than the persistence length. In this language, at constant interfacial area, the swellability of a middle-phase microemulsion is determined by the dispersion size.

A related question is: Why is a lamellar phase also sometimes found to exhibit a limited swellability [46,58]? Is this limited swellability caused by defects? Or is it necessary to invoke attractions between the surfactant monolayers? If attractions are responsible, classical van der Waals attraction is not a very good candidate, as it is found that the thickness of the water and oil layers is so great (several tens of nanometers) and the Hamaker constant for O/W layers is so small that van der Waals attraction seems to be too weak.

ACKNOWLEDGMENTS

The contribution of WKK to the work presented here was made possible by a fellowship of the Royal Netherlands Academy of Arts and Sciences.

REFERENCES

1. J. H. Schulman and E. G. Cockbain, *Trans. Faraday Soc.* 36:551 (1940).
2. T. P. Hoar and J. H. Schulman, *Nature* 152:102 (1943).
3. J. E. Bowcott and J. H. Schulman, *Z. Electrochem.* 59:283 (1955).
4. G. J. Verhoeckx, P. L. de Bruyn, and J. Th. G. Overbeek, *J. Colloid Interface Sci.* 119:409 (1987).
5. W. K. Kegel, G. A. van Aken, M. N. Bouts, H. N. W. Lekkerkerker, J. Th. G. Overbeek, and P. L. de Bruyn, *Langmuir* 9:252 (1993).
6. H. Saito and K. Shinoda, *J. Colloid Interface Sci.* 32:647 (1970).
7. P. A. Winsor, *Trans. Faraday Soc.* 44:376 (1948).

8. P. A. Winsor, *Solvent Properties of Amphiphilic Compounds*, Butterworth, London, 1954, pp. 7, 57–60, 68–71, 190.
9. P. A. Winsor, *Chem. Rev.* 68:1 (1968).
10. L. R. Angel, D. F. Evans, and B. W. Ninham, *J. Phys. Chem.* 87:538 (1983).
11. M. L. Robbins, in *Micellization, Solubilization and Microemulsions*, Vol. 2, (K. L. Mittal, ed.), Plenum, New York, 1977, p. 713.
12. J. Th. G. Overbeek, *Kon. Ned. Akad. Wetenschap. Proc. B* 89:66 (1986).
13. W. Helfrich, *Z. Naturforsch.* 28c:693 (1973).
14. D. A. Huse and S. Leibler, *J. Phys. (France)* 49:605 (1988).
15. J. Th. G. Overbeek in *Surfactants in Solution*, Vol. 11 (K. L. Mittal and D. O. Shah, eds), Plenum, New York, 1991, p. 3.
16. P. L. de Bruyn, J. Th. G. Overbeek, and G. J. Verhoeckx, *J. Colloid Interface Sci.* 127:244 (1989).
17. Y. Talmon and S. Prager, *Nature* 267:333 (1977).
18. P. G. de Gennes and C. Taupin, *J. Phys. Chem.* 86:2294 (1982).
19. J. Jouffroy, P. Levinson, and P. G. de Gennes, *J. Phys. (France)* 43:1241 (1982).
20. D. Andelman, M. E. Cates, D. Roux, and S. A. Safran, *J. Chem. Phys.* 87:7229 (1987).
21. J. C. Wheeler and B. Widom, *J. Am. Chem. Soc.* 90:3064 (1968).
22. B. Widom, *J. Chem. Phys.* 84:6943 (1986).
23. Y. Levin and K. A. Dawson, *Phys. Rev. A* 42:1976 (1990).
24. B. Widom, *Ber. Bunsenges. Phys. Chem.* 100:242 (1996).
25. G. Gompper, *Ber. Bunsenges. Phys. Chem.* 100:264 (1996).
26. J. Th. G. Overbeek, *Prog. Colloid Polym. Sci.* 83:1 (1990).
27. W. K. Kegel and H. Reiss, *Ber. Bunsenges. Phys. Chem.* 100:300 (1996). Erratum: 101:1963 (1997).
28. J. Th. G. Overbeek, G. J. Verhoeckx, P. L. de Bruyn, and H. N. W. Lekkerkerker, *J. Colloid Interface Sci.* 119:422 (1987).
29. D. C. Morse and S. T. Milner, *Europhys. Lett.* 26:565 (1994).
30. K. M. Palmer and D. C. Morse, *J. Chem. Phys.* 105:11147 (1996).
31. H. Reiss, W. K. Kegel, and J. Groenewold, *Ber. Bunsenges. Phys. Chem.* 100:279 (1996).
32. J. Th. G. Overbeek, *Faraday Disc. Chem. Soc.* 65:7 (1978).
33. H. Reiss and W. K. Kegel, *J. Phys. Chem.* 100:10428 (1996).
34. H. Reiss, W. K. Kegel, and J. L. Katz, *Phys. Rev. Lett.* 78:4506 (1997).
35. M. E. Fisher, *Physics* 3:255 (1967).
36. A. Dillman and G. E. A. Meier, *J. Chem. Phys.* 94:3872 (1991).
37. V. I. Kalikmanov and M. E. H. van Dongen, *Phys. Rev. E* 51:4391 (1995).
38. W. Cai, T. C. Lubenski, P. Nelson, and T. Powers, *J. Phys. II (France)* 4:931 (1994).
39. M. Borkovec, *J. Chem. Phys.* 91:6268 (1989).
40. J. C. Eriksson and S. Ljunggren, *Prog. Colloid Polym. Sci.* 83:41 (1990).
41. S. T. Milner and T. A. Witten, *J. Phys. (France)* 49:1951 (1988).
42. A. N. Stokes, *J. Chem. Phys.* 65:261 (1976).
43. H. N. W. Lekkerkerker, *Physica A* 159:319 (1989).
44. H. N. W. Lekkerkerker, *Physica A* 167:384 (1990).
45. J. Meunier, *J. Phys. Lett. (France)* 46:L-1005 (1985).
46. B. P. Binks, H. Kelay, and J. Meunier, *Europhys. Lett.* 16:53 (1991).
47. L. T. Lee, D. Langevin, J. Meunier, K. Wong, and B. Cabane, *Prog. Colloid Polym. Sci.* 81:209 (1990).
48. H. Kelay, J. Meunier, and B. P. Binks, *Phys. Rev. Lett.* 70:1485 (1993).
49. F. Sicoli and D. Langevin, *J. Chem. Phys.* 99:4759 (1993).
50. W. K. Kegel, I. Bodnar, and H. N. W. Lekkerkerker, *J. Phys. Chem.* 99:3272 (1995).
51. J. C. Eriksson and S. Ljunggren, *Langmuir* 11:1145 (1995).
52. M. Gradzielski, D. Langevin, and B. Farago, *Phys. Rev. E* 53:3900 (1996).
53. W. K. Kegel, *Langmuir* 13:873 (1997).
54. R. Aveyard, B. P. Binks, and J. Mead, *J. Chem. Soc., Faraday Trans.* 82:1755 (1986).

55. G. A. van Aken, A study of Winsor II microemulsion equilibria, Doctor's Thesis, University of Utrecht, 1990.
56. M. Almgren, R. Johansson, and J. C. Eriksson, *J. Phys. Chem.* 97:1993 (1993).
57. H. Kellay, Y. Hendrikx, J. Meunier, and B. P. Binks. *J. Phys. II* 3:1747 (1993).
58. W. K. Kegel and H. N. W. Lekkerkerker, *J. Phys. Chem.* 97:11124 (1993).
59. R. Strey, J. Winkler, and L. Magid, *J. Phys. Chem.* 95:7502 (1991).